Positive exchange-bias induced by interface domain wall quenching in GdFe/TbFe films

Yves Henry*
Institut de Physique et Chimie des Matériaux de Strasbourg, CNRS and Université Louis Pasteur, BP 43, F-67034 Strasbourg Cedex 2, France

Stéphane Mangin, Thomas Hauet, and François Montaigne
Laboratoire de Physique des Matériaux, Université Henri Poincaré, BP 239, F-54506 Vandoeuvre-les-Nancy Cedex, France
(Received 19 September 2005; revised manuscript received 2 February 2006; published 21 April 2006)

Exchange-bias in a soft/hard ferrimagnetic (sFi/hFi) GdFe/TbFe bilayer with antiferromagnetic interface coupling has been studied as a function of the magnitude H_{cf} and angle ψ_{cf} of the cooling field. A continuous transition from negative exchange bias to positive exchange bias is observed with increasing H_{cf}. The transition is shown to arise from a *progressive* rotation of the direction of the interfacial pinning acting on the sFi magnetization in the plane of the film. This is explained by the presence of a partial interface domain wall (iDW) quenched in the hFi layer, the thickness and angular span of which depend on H_{cf}. The presence of the frozen iDW at the end of cooling is clearly evidenced thanks in particular to the strong effect a change of its handedness produces on the ψ_{cf} dependence of the exchange-bias field H_E. Overall, H_E is shown to be uniquely determined by the orientation of the hFi magnetization at the interface, whereas the coercivity of the sFi layer proves to be dependent also on the detailed micromagnetic structure deeper in the hFi layer.

DOI: 10.1103/PhysRevB.73.134420 PACS number(s): 75.70.Cn, 75.30.Gw, 73.43.Qt, 75.60.Ch

I. INTRODUCTION

Conventional exchange-bias (EB) results from the exchange coupling of a ferromagnet (F) to an antiferromagnet (AF) across their common interface. It appears generally after the F/AF structure has been cooled through the blocking temperature T_B of the AF material in a magnetic field. Positive exchange-bias (PEB)[1,2] refers to a situation where the ferromagnetic hysteresis loop is shifted along the field axis by a positive amount H_E, that is by convention, in the direction of the magnetic field $\mathbf{H}_{cf}$ applied during cooling. This is contrary to what is observed for most exchange-biased systems: In the usual situation referred to as negative exchange bias (NEB), the magnetization loop is shifted negatively ($H_E<0$), in the direction opposite to that of $\mathbf{H}_{cf}$.[3,4]

It has been recognized that the occurrence of PEB in F/AF systems requires that (i) the interface AF spins carry a net magnetization $\mathbf{M}_{AF}^{i}$ so as to couple to $\mathbf{H}_{cf}$ during cooling through T_B and that (ii) the interfacial exchange interaction between the F and AF materials be of antiferromagnetic nature.[1,5–7] In these conditions, a competition takes place between the Zeeman interaction and the interfacial exchange interaction which both act on the interface AF spins. For small applied fields, the orientation of $\mathbf{M}_{AF}^{i}$ is determined by the exchange interaction with the F layer: It is oriented oppositely to the F magnetization, hence antiparallel to $\mathbf{H}_{cf}$. For large applied fields, the Zeeman interaction overcomes the interfacial exchange coupling and $\mathbf{M}_{AF}^{i}$ aligns parallel to $\mathbf{H}_{cf}$. On the basis of these simple energetic arguments, one may predict that a transition from NEB at small H_{cf} to PEB at large H_{cf} should occur.[1] It is expected to be abrupt in ideal F/AF bilayers. In practice, however, it has never been found so.

Because of the existence of spatial inhomogeneities in the real F/AF samples, the NEB to PEB transition may take two distinct forms depending on the relative sizes of the magnetic domains in the F and AF layers.[8] (i) In bilayer samples where the AF domains are smaller than the F ones, exchange bias is averaged in direction and magnitude over several AF domains. This usually leads to a single hysteresis loop whose shift varies continuously as a function of H_{cf}. This is the behavior encountered most frequently.[1,5–7] Here, the continuous character of the transition from NEB to PEB has an *extrinsic* origin since it is related to imperfections. (ii) When, on the contrary, the size of the AF domains is comparable or larger than that of the F domains, no averaging of EB occurs. Then, only the sign of the exchange-bias field, not its amplitude, depends on the cooling field. An intermediate regime exists between pure NEB at small H_{cf} and pure PEB at large H_{cf} in which double hysteresis loops are observed.[8]

Recently, positive exchange bias as well as a smooth variation from NEB to PEB with increasing cooling field have been reported for another type of system, employing neither ferromagnetic nor antiferromagnetic materials: The soft/hard $Gd_{40}Fe_{60}/Tb_{12}Fe_{88}$ (sFi/hFi) bilayer system, in which both constituents are amorphous ferrimagnetic alloys.[9] This system possesses the aforementioned properties necessary for the occurrence of PEB. First, a net magnetic polarization of the interface spins exists inherently so that they naturally sense $\mathbf{H}_{cf}$. Second, the interfacial coupling between the $Gd_{40}Fe_{60}$ and $Tb_{12}Fe_{88}$ alloys is antiferromagnetic. For such sFi/hFi stacks with thickness of the individual layers of several tens of nanometers, it has been shown that a parallel-to-plane interface domain wall (iDW) extending in both sFi and hFi slabs forms at room temperature whenever a strong magnetic field is applied in order to bring the net magnetizations of the two materials parallel to each other. Moreover, it has been suggested that the portion of the iDW located in the $Tb_{12}Fe_{88}$ (hFi) pinning layer might freeze upon cooling to low temperature and that the variation of H_E with H_{cf} might

closely reflect field-induced changes in the direction of the frozen interface hFi magnetization.

In the present contribution, we bring clear evidence that a partial iDW is indeed quenched in the hFi, after field cooling to low temperature, by analyzing the variation of the exchange-bias field H_E with the angle of the cooling field ψ_{cf} (Sec. IV B). In particular, we show that reversing the handedness of the iDW formed at elevated temperature strongly affects the angular variation of H_E. But in the first place, we demonstrate (Sec. IV A) that the observed continuous change from NEB to PEB with increasing H_{cf} is an *intrinsic* phenomenon for the $Gd_{40}Fe_{60}/Tb_{12}Fe_{88}$ system: It is related to a progressive rotation of the direction of the interfacial pinning acting on the sFi magnetization, from parallel to $\mathbf{H}_{cf}$ as H_{cf} tends to zero, to antiparallel to $\mathbf{H}_{cf}$ as H_{cf} tends to infinity. This rotation is ascribed to a just as progressive decrease in the thickness and angular span of the partial iDW quenched in the hFi layer. Finally, we show that the exchange-bias field H_E depends solely on the orientation of the interface hFi magnetization (Sec. IV C), whereas the coercivity of the sFi layer H_C depends on the orientation of the interface magnetization *and* on the details of the bulk micromagnetic structure of the hFi material (Sec. IV D).

II. SAMPLE DESCRIPTION AND ROOM TEMPERATURE BEHAVIOR

The sample studied here consists of a $Gd_{40}Fe_{60}$(100 nm)/$Tb_{12}Fe_{88}$(50 nm) bilayer fabricated by high vacuum co-evaporation of the pure elements on a glass substrate kept at liquid nitrogen temperature.[9] It is protected against oxidation by a 30-nm-thick highly resistive Si layer. The amorphous $Gd_{40}Fe_{60}$ and $Tb_{12}Fe_{88}$ alloys, thereafter referred to as GdFe and TbFe, are ferrimagnetic: The magnetization of the rare-earth sublattice is antiparallel to that of the Fe sublattice. In the entire range of temperature of interest in this work (20–295 K), the dominant sublattice magnetization is that of the rare earth in GdFe and that of Fe in TbFe. Then, according to Mergel's nomenclature,[10] our sample is an exchange-coupled double layer (ECDL) of type A. In its ground state, the net magnetizations of the two layers are maintained antiparallel to each other, essentially as a result of the continuity of the exchange coupling through the Fe sublattices across the interface. GdFe and TbFe are naturally magnetized in plane. Moreover, the specific geometry employed for the deposition[11] is at the origin of a well defined uniaxial anisotropy of easy axis $\pm\hat{\mathbf{u}}$, in the plane of the GdFe layer.

To investigate the exchange-bias properties of our system, we carried out anisotropic magnetoresistance (AMR) measurements in the usual current-in-plane geometry, applying the conventional four wire method with a direct bias current of 5 mA. The direction of the electrical current $\hat{\mathbf{i}}$ was colinear to $\hat{\mathbf{u}}$, as was systematically the cycling field $\mathbf{H}$. To illustrate the experimental technique employed and introduce the magnetic behavior of the system at room temperature, we present in Fig. 1 the resistance versus field $R(H)$ loop of the sample and, for comparison, the corresponding magnetization loop. The various magnetic configurations adopted as a function of H are well known from previous works on this particular GdFe/TbFe system,[9] as well as on many equivalent ECDL systems.[10,12,13] They are shown schematically in Fig. 1(a) and can be summarized as follows.

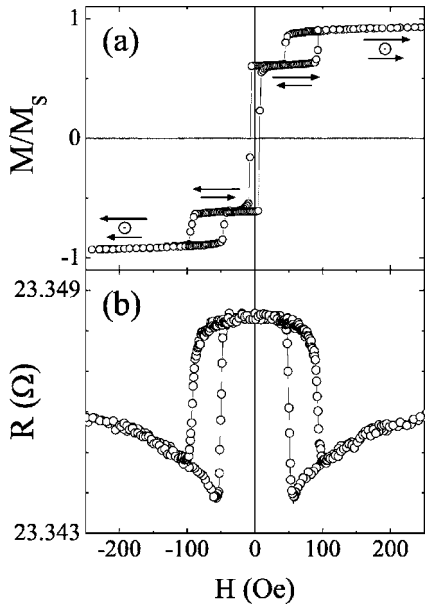

FIG. 1. Room temperature magnetization (a) and AMR (b) loops measured with the external field applied along the easy axis of the GdFe layer. (a) The dotted circles in the sketches of the magnetic configurations indicate the presence of a parallel-to-interface magnetic domain wall.

(i) In small applied fields ($|H|<50$ Oe typically), the net magnetizations of the two ferrimagnetic layers are uniform throughout the thickness, colinear to $\mathbf{H}$, and, as a result of the antiferromagnetic interfacial coupling, antiparallel to each other. The magnetization of that of the two layers with the largest magnetic moment (GdFe) is aligned parallel to the applied field (neglecting the narrow hysteresis around zero field). Note that the simultaneous reversals of the GdFe and TbFe magnetizations which occur at field values very close to zero do not show up in the $R(H)$ data since they produce no change in the orientation of the magnetization with respect to the direction of the measurement current. Furthermore, the magnetization in both layers remaining colinear to $\hat{\mathbf{i}}$, the sample resistance takes on a maximum and (almost) constant value.

(ii) In large applied fields ($|H|>100$ Oe typically), the magnetizations of the two ferrimagnets are forced to align more or less parallel to each other. However, as a result of the competing effects of the Zeeman interaction and antiferromagnetic interfacial exchange interaction, the two layers are no longer magnetically uniform: A parallel-to-plane domain wall forms which encompasses the interface (Fig. 2). Although it extends in both materials, the iDW primarily lies in TbFe because of its lower exchange energy and net magnetization.[9] The magnetization distribution thus acquires a significant transverse component (perpendicular to $\mathbf{H}$, $\hat{\mathbf{u}}$, and $\hat{\mathbf{i}}$), which leads to a reduced resistance of the sample. With increasing (respectively decreasing) field magnitude, the iDW suffers a progressive compression (respectively de-

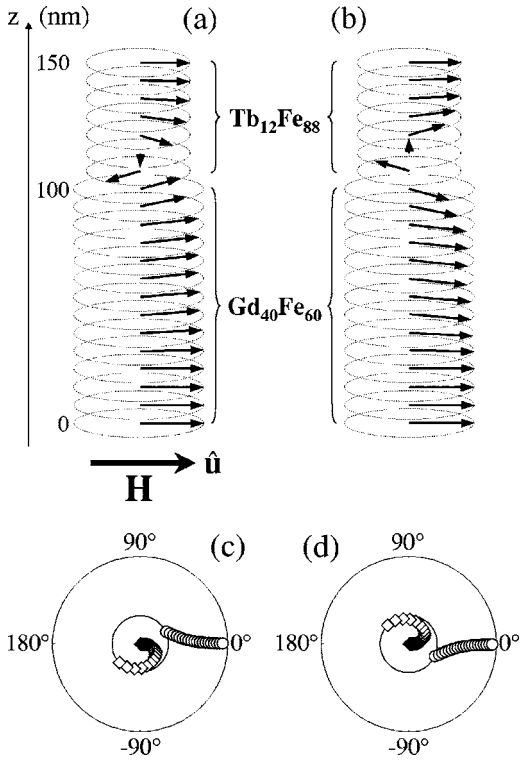

FIG. 2. (a), (b) Schematic representations of the interface domain walls formed in the $Gd_{40}Fe_{60}(100\ nm)/Tb_{12}Fe_{88}(50\ nm)$ bilayer, at room temperature. Shown are the energetically equivalent (a) right handed wall and (b) left handed wall (see Sec. III A for details). (c), (d) Polar plots of the depth dependence of the magnetization azimuthal angle in the interface domain walls sketched in (a), (b). Diamonds and circles correspond to TbFe and GdFe, respectively.

compression), i.e., its thickness decreases (respectively increases). Interestingly, this (de)compression process, which is completely reversible, appears much more clearly in the $R(H)$ curve [Fig. 1(b)] than in the $M(H)$ one [Fig. 1(a)]. In the latter, indeed, it manifests by a very slow approach to saturation, hardly discernible at first sight, whereas in the former it gives rise to a strong concave curvature.

III. EXPERIMENTAL PROCEDURES AND MODELING

A. Experimental procedures

Two types of experiments with different purposes were carried out in the present work. They differ by the magnetic history of the sample prior to the measurements. Before describing them in detail, it is necessary to draw the reader's attention to the following point. The symmetry of our system is such that two different iDWs may form at room temperature when, starting from zero field, i.e., antiparallel alignment of the GdFe and TbFe net magnetizations, a large magnetic field is applied along $\hat{\mathbf{u}}$. These are energetically equivalent, of opposite handedness, and mirror symmetric from one another about $\hat{\mathbf{u}}$ (Fig. 2). It is possible to promote the formation of one particular iDW by setting the field not exactly parallel to $\hat{\mathbf{u}}$ but at a small angle ϵ from it, either positive or negative. This allows one to select that of the two magnetic configurations whose overall transverse (perpendicular to $\hat{\mathbf{u}}$) component of magnetization is parallel to the transverse component of the applied field. We will refer to these two types of iDW as "left handed" or "right handed" depending on whether the TbFe magnetization rotates clockwise or counterclockwise with increasing distance from the GdFe/TbFe interface (Fig. 2).

In the first type of experiment (type I) designed to elucidate the origin of the transition from NEB to PEB, the orientation of the cooling field was fixed and its magnitude was varied. Thus, the thickness and shape of the frozen iDW are expected to change. The following procedure was used. First, the largest possible field of 12 kOe available in our experimental setup was applied at room temperature, along the easy direction $+\hat{\mathbf{u}}$. This direction was arbitrarily chosen and will be considered all along this paper as the positive field direction for $\mathbf{H}$. Note that by applying the field as closely as practically possible from the easy axis, no selection of the iDW handedness could be performed. Next, the field strength was reduced to H_{cf} (with $0 \leqslant H_{cf} \leqslant 12$ kOe), which allowed the iDW formed to decompress: The smaller H_{cf} the thicker the wall. Finally, the sample was cooled down to 20 K, a temperature sufficiently low so that TbFe becomes extremely hard magnetically and its magnetization distribution freezes, owing to a huge increase of its (local) magnetic anisotropy (the mechanism of freezing of the TbFe magnetization is discussed at the end of Sec. IV A 2).

In the second type of experiment (type II), whose purpose was to bring an undisputable evidence of the presence of a partial iDW quenched in TbFe, the magnitude of the cooling field was set to a constant value of 10 kOe and its angle ψ_{cf} with respect to the easy direction $+\hat{\mathbf{u}}$ was varied. Here, care was taken to select either a left handed iDW or a right handed iDW by applying initially the maximum field of 12 kOe at $\epsilon = +2°$ or $\epsilon = -2°$ from $+\hat{\mathbf{u}}$. Having selected the desired kind of iDW, the external field was then decreased to $H_{cf} = 10$ kOe and rotated to a given angular position ψ_{cf}. The external field still being extremely large, this essentially produced a block-wise rotation of the magnetic configuration just formed, as will be ascertained later in this paper. Finally, the sample was cooled to 20 K. With this procedure, only the average orientation of the frozen TbFe magnetization is expected to differ from one experiment to the next, not the thickness and global shape of the quenched iDW.

The sequence of resistivity measurements carried out after stabilization of the temperature to 20 K, which will be described now, aimed at determining the exchange-bias field and the effective direction of the interfacial pinning acting on the sFi magnetization *independently* from one another, yet in the very same experimental conditions. This sequence was strictly identical for the two types of experiments (I and II) and contained two sorts of measurements.

(i) First, resistance versus field $R(H)$ *minor* loops of the soft material were measured by cycling the applied field along $\pm\hat{\mathbf{u}}$. Several loops (up to six) were taken, i.e., the sFi magnetization was reversed back and forth several times, to allow the hFi magnetization close to the interface to rearrange,[9] should a rearrangement arise, and reach a configuration reproducible upon additional sFi reversals. As the

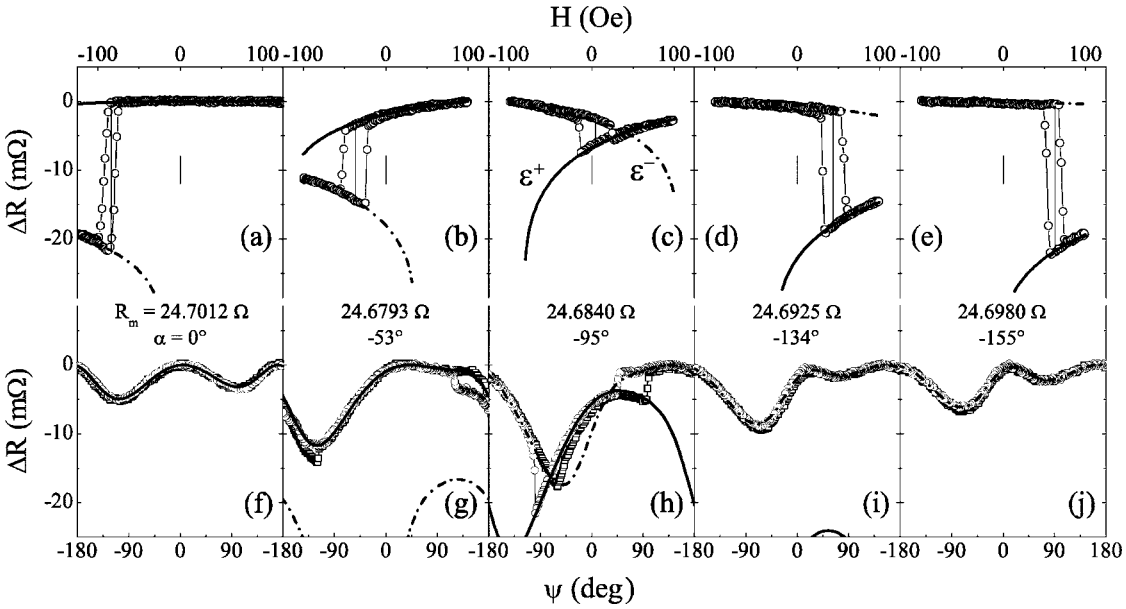

FIG. 3. Examples of experimental (symbols) and theoretical (thick lines) AMR variations $\Delta R = R - R_m$ as a function of the cycling field magnitude H (a)–(e) and the rotating field angle ψ (f)–(j), for varying values of the cooling field (experiments of type I): (a), (f) H_{cf} =40 Oe, (b), (g) H_{cf}=250 Oe, (c), (h) H_{cf}=1 kOe, (d), (i) H_{cf}=3 kOe, (e), (j) H_{cf}=12 kOe. R_m is the corresponding maximum of resistance measured when varying ψ between −180° and +180°. Circles and squares in (f)–(j) correspond, respectively, to the counterclockwise and clockwise directions of rotation of $\mathbf{H_{rot}}$, whereas thick solid lines and dashed lines correspond, respectively, to magnetic configurations of type ε^+ and type ε^- (see Sec. III B for details). The theoretical data were obtained assuming a small angle of +1.5° between $\hat{\mathbf{i}}$ and $\hat{\mathbf{u}}$, and using the pinning angles α indicated.

largest part of the irreversible rearrangement of the hFi magnetization, when any, was triggered by the very first reversal of GdFe, reproducibility of the $R(H)$ loop shape and reversal fields was most often achieved from the second cycle onwards. On very few occasions, it took up to three cycles before no more change could be observed. In the case of the bilayer studied here, the initial reorganization of the TbFe magnetization was always limited, as attested by the moderate changes in resistance observed.[14] However, much more important reorganizations have been evidenced by standard magnetometry[9] and polarized neutron reflectometry[15] in other samples of the same nominal composition. Note that the exchange-bias field H_E was systematically determined from the very last minor loop recorded [Figs. 3(a)–3(e)].

(ii) Second, the field was set to a constant value of H_{rot} =−50 Oe [decreasing field branch of the $R(H)$ loop] and rotated 360° successively counterclockwise and clockwise, while constantly monitoring the sample resistance [Figs. 3(f)–3(j)]. For the sake of consistency, the field angle ψ was defined as 0 for $\mathbf{H_{rot}}$ parallel to $+\hat{\mathbf{u}}$, which was realized halfway in each of the field revolutions. Such a small field as H_{rot} induces tiny, vertically nonuniform and essentially reversible magnetization rotations in the sFi slab.[16] As a consequence, with few exceptions such as the one shown in Fig. 3(h), which will be discussed later in the paper, only very little rotational hysteresis could be detected in these rotating field experiments, which are perturbative in nature.[17] The shape and peak-to-peak amplitude of the $R(\psi)$ curves depend sensitively on the orientation of the interfacial pinning direction $\hat{\mathbf{a}}$ with respect to the positive field direction $+\hat{\mathbf{u}}$. Owing to this property, it is possible to determine accurately the so-called pinning angle α between $\hat{\mathbf{a}}$ and $+\hat{\mathbf{u}}$ from the $R(\psi)$ data.

In fact, such a dependency exists also for the $R(H)$ loops so that accurate information regarding the pinning angle may be obtained from these data, too. The rotating field experiments might then appear as superfluous. However, the geometry of our experiments is such $(\mathbf{H}\|\hat{\mathbf{i}}\|\hat{\mathbf{u}})$ that a given pinning angle α and the opposite angle $-\alpha$ give rise to strictly identical $R(H)$ loops. As a consequence, only the absolute value of α can be determined from the $R(H)$ data. A similar ambiguity does not exist for the $R(\psi)$ curves. But above all, the rotating field measurements make possible a determination of α which is totally independent from that of the exchange-bias field H_E.

B. Micromagnetic model

The micromagnetic model used to reproduce the experimental data and extract the value of α is extremely simple. This is a one-dimensional atomic model like many others used successfully in the past, in studies of exchange-coupled multilayers,[18] and thin film exchange-spring magnets.[19,20] In its details, our model is similar to the one employed in Ref. 9, with the only difference that, in the present case, the TbFe layer is assumed to be perfectly rigid magnetically so that it does not give rise to any change in resistance upon rotation or reversal of the applied field. A description of the frozen magnetic configuration(s) considered for TbFe at low temperature will be given in due course, later in this paper. The GdFe layer is treated as a chain of (200) spins running normal to the hFi/sFi interface. Its total magnetic energy con-

TABLE I. Electrical properties of the $Gd_{40}Fe_{60}$ and $Tb_{12}Fe_{88}$ amorphous alloys at 20 K; $\rho_\parallel$ (respectively $\rho_\perp$) is the resistivity when the magnetization is parallel (respectively perpendicular) to the current.

	$Gd_{40}Fe_{60}$	$Tb_{12}Fe_{88}$
$\rho_\parallel$ ($\mu\Omega$ cm)	336	186
$(\rho_\parallel-\rho_\perp)/\rho_\parallel$	3.2×10^{-3}	4.6×10^{-3}

taining exchange, anisotropy, and Zeeman terms is minimized numerically to determine its (meta)stable magnetic configuration(s), as a function of ψ and H. These have the form of magnetization profiles, entirely described by the depth dependence of the magnetization azimuthal angle $\theta(z)$ with respect to $+\hat{\mathbf{u}}$ ($\hat{\mathbf{i}}$). The electrical resistance is evaluated for comparison with the experimental data, assuming that the resistivity of both GdFe and TbFe alloys locally obeys $\rho(z)=\rho_\parallel\cos^2\theta(z)+\rho_\perp\sin^2\theta(z)$ and integrating over the whole thickness of the bilayer.[19,21–23] The longitudinal resistivities $\rho_\parallel$ and AMR ratios $(\rho_\parallel-\rho_\perp)/\rho_\parallel$ used in the computation are given in Table I. They are consistant with results from complementary measurements carried out on single $Gd_{40}Fe_{60}$ and $Tb_{12}Fe_{88}$ layers.

As a limit condition, the interface TbFe spin is supposed here to make an angle $\theta^i_{\mathrm{TbFe}}=\alpha\pm180°$ (see Ref. 24) with the easy direction $+\hat{\mathbf{u}}$. This angle is adjusted so as to obtain the best possible agreement between experimental and calculated AMR data. Since we consider the TbFe magnetization as quenched, the only parameters controlling the magnetic behavior of the system are, besides α, the saturation magnetization $M=1000$ emu/cm^3, the anisotropy constant $K=10^5$ erg/cm^3, and the bulk exchange stiffness $A=6\times10^{-7}$ erg/cm of GdFe (at 20 K), and the exchange coupling across the GdFe/TbFe interface $J=-7$ erg/cm^2. The first three of them (M, K, and A) are known from previous studies.[9,22,25] The value of the last one (J) proved to have little influence on the computed $R(\psi)$ curves. It was adjusted so that our model could account for the exchange-bias field of -84 Oe measured in the case where $H_{cf}<50$ Oe ($\psi_{cf}=0°$), which corresponds to $\alpha=0°$ (see below). It was kept fixed in all the other cases.

In spite of its simplicity, the model allows one to reproduce the measured data accurately. In particular, the nontrivial shape of the $R(\psi)$ curves [Figs. 3(f)–3(j)] resulting from the combination of two magnetic anisotropies of different axes and symmetries (uniaxial and unidirectional) but of comparable magnitudes is accounted for. Our confidence in the validity of the model and in the values of the pinning angle deduced from it is further reinforced by the fact that the very same values, or values extremely close to them, allow one to simulate also the measured $R(H)$ loops [Figs. 3(a)–3(e)]. The remarkable agreement between experiments and simulations indicates that the assumption we made of a rigid TbFe magnetization is a reasonable one, at least in first approximation. It is also a strong indication that, in the vast majority of the experiments reported and with the exceptions of the particular conditions where irreversible transitions take place, the bilayer studied behaves essentially as a perpendicular-to-interface chain of spins, i.e., in a laterally (in-plane) uniform manner, as assumed in the model. The possibility that the TbFe magnetization be broken into a magnetic multi-domain state can thus be ruled out, in general.

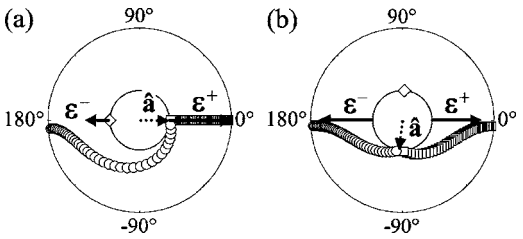

FIG. 4. Polar plots of the theoretical depth dependence of the magnetization azimuthal angle in GdFe, at $H=H_E$ (20 K), for two values of the cooling field (experiments of type I): (a) $H_{cf}=40$ Oe [$H_E=-84$ Oe, Fig. 3(a)] and (b) $H_{cf}=1$ kOe [$H_E=+5$ Oe, Fig. 3(c)]. Circles and squares correspond to the ε^- and ε^+ magnetic configurations, respectively. The diamonds and the dotted arrows indicate the angle of the frozen TbFe interface magnetization θ^i_{TbFe} and the direction of pinning $\hat{\mathbf{a}}$. The solid arrows represent the overall longitudinal magnetization components of the GdFe magnetic profiles (see Sec. III B for details).

C. Low temperature magnetic configurations

Our micromagnetic model shows that in moderate fields, such as those applied during the reported experiments, there exist (at the most) two stable magnetic configurations accessible for the exchange-biased GdFe layer.[26] One of them corresponds (always) to the ground state, the other one to a metastable state (whenever it exists). These magnetic configurations mainly differ from one another in that their overall longitudinal (colinear to $\hat{\mathbf{u}}$) magnetization components $\mathbf{M_L}$ are systematically antiparallel to each other (Fig. 4). This property is at the origin of a possible classification, which will be adopted in the present paper, of the stable magnetic configurations in two different types: Those configurations where $\mathbf{M_L}$ is parallel to $+\hat{\mathbf{u}}$ will be called of type ε^+, those where $\mathbf{M_L}$ is parallel to $-\hat{\mathbf{u}}$ of type ε^-. In the case of the cycling field measurements [Figs. 3(a)–3(e)], it was naturally expected that the relative stability of the ε^+ and ε^- configurations would change with varying H (the state of lowest energy becoming the one of highest energy and vice versa) and that the system would undergo irreversible transitions at some points corresponding to the reversal of the sFi magnetization. In the case of the rotating field measurements, irreversible transitions between the ε^+ and ε^- states were undesirable, as are all irreversible processes in perturbative measurements.[17] Although the magnitude of $\mathbf{H_{rot}}$ was taken small so as to prevent their occurrence in as many situations (i.e., for as many values of α) as possible, transitions occurred in some measurements [Fig. 3(h)], giving rise to significant rotational hysteresis. All of these measurements corresponded to cases where $|\alpha|$ was close to 90°. Such a situation makes irreversible magnetization processes hardly avoidable in practice, no matter how small the rotating field is.

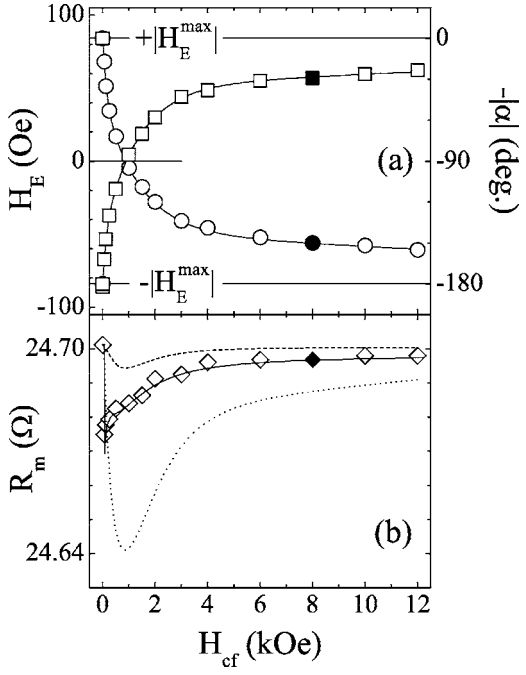

FIG. 5. (a) Exchange-bias field H_E (squares), pinning angle α (circles), and (b) maximum resistance R_m (diamonds) as a function of the cooling field H_{cf} (experiments of type I), at 20 K. The open and solid symbols correspond to cases where α was found negative and positive, respectively. The lines in (b) are theoretical predictions (see Sec. IV A 2 for details), those in (a) are guides to the eye.

As illustrated in Fig. 4, the stable magnetic configurations of GdFe at low temperature most often consist of spiral profiles, in which the magnetization rotates progressively from the pinning direction to the external field direction with increasing distance from the interface. As H varies, these profiles, very much like the iDW formed at room temperature, undergo some kind of (de)compression. This manifests by a curvature in the corresponding part of the $R(H)$ loop (Fig. 3), whose importance scales with the degree of magnetization twisting in the profile. The difference in the amount of curvature in the leftmost (ε^- state) and rightmost (ε^+ state) branches of the AMR loop, as well as in their mean resistance level, is a direct indication of the orientation of the pinning direction $\hat{\mathbf{a}}$ with respect to $\mathbf{H}$ and $\hat{\mathbf{u}}$. For $|\alpha|$ close to 90°, for instance, the ε^+ and ε^- configurations are necessarily approximately mirror symmetric from one another about the hard axis of magnetization [Fig. 4(b)] and so are the left and right branches about the resistance axis [Fig. 3(c)]. The AMR contrast between the ε^- and ε^+ states is then particularly weak.

IV. RESULTS AND DISCUSSION

A. Exchange-bias properties versus cooling field magnitude

1. Exchange-bias field and pinning angle

Let us now focus on the results of the experiments of type I. Figure 5(a) shows the variations of the exchange-bias field H_E and of the interfacial pinning angle α as a function of the cooling field magnitude H_{cf}. It illustrates the fact that the GdFe/TbFe system exhibits a continuous variation from NEB at small H_{cf} to PEB at large H_{cf}.[9] For the particular bilayer studied here, the crossover takes place at $H_{cf}^{*}=0.9$ kOe. From Fig. 5(a), it is obvious that a strong geometrical correlation exists between H_E and $|\alpha|$. We will discuss it in more detail in Sec. IV C. At this point, we just note that H_E takes on a maximum negative value of $-|H_E^{max}|=-84$ Oe for $|\alpha|=0°$ and that it tends towards a maximum positive value of $+|H_E^{max}|$ as $|\alpha|$ approaches 180°. The crossover at H_{cf}^{*} corresponds precisely to the passage from $|\alpha|<90°$ to $|\alpha|>90°$. More generally, we see that the variation of H_E reflects a progressive rotation of the pinning direction further and further away from the cooling field direction as H_{cf} increases: $\hat{\mathbf{a}}$ goes continuously from parallel to $\mathbf{H}_{cf}$, for H_{cf} close to zero, towards antiparallel to $\mathbf{H}_{cf}$, as H_{cf} tends to infinity.

The interfacial coupling between GdFe and TbFe being antiferromagnetic, it is extremely tempting to relate the motion of $\hat{\mathbf{a}}$ to the rotation of the interface hFi magnetization towards the applied field direction and to the concomitant compression of the partial iDW present in TbFe, which are known to occur as the external field strength is increased, at elevated temperature (see Sec. II). However, before taking this step, evidence should be given that a memory of the twisted magnetic configuration formed in TbFe before field cooling is maintained after cooling.

2. Maximum resistance

One piece of evidence is provided through the variation of R_m with H_{cf} [Fig. 5(b)], where R_m is the largest resistance that the sample assumed during the rotating field measurements, i.e., the maximum of the $R(\psi)$ curve. One may immediately notice that a strong similarity exists between the $R_m(H_{cf})$ dependence and the room temperature $R(H)$ loop of Fig. 1(b). R_m is naturally related to the magnetic states of the two constituents of the bilayer, since both of them exhibit AMR (Table I). It is then likely to depend on H_{cf} in two ways, *a priori* equally important and not totally uncorrelated. (i) R_m will necessarily depend on H_{cf} because the "unperturbed" magnetic configuration of GdFe, in which $\mathbf{H}_{\mathbf{rot}}$ induces little reversible rotations, is strongly determined by α, which surely varies with H_{cf}. (ii) It is also susceptible to depend on H_{cf} if, as we wish to demonstrate, the whole magnetic configuration frozen in TbFe changes with H_{cf} and not just the one at the interface ($\theta_{\mathrm{TbFe}}^{i}$).

The discontinuous lines in Fig. 5(b) are the theoretical variations of R_m as a function of H_{cf} predicted by our model on the following two assumptions: (i) Except at the interface where $\theta_{\mathrm{TbFe}}^{i}=\alpha\pm180°$, no change occurs in the micromagnetic structure of TbFe whose magnetization always lies at $\theta(z)=0°$, along the cooling field direction (dashed line); (ii) TbFe is magnetized uniformly at $\theta(z)=\theta_{\mathrm{TbFe}}^{i}=\alpha\pm180°$ (dotted line). Obviously, neither the shape of the $R_m(H_{cf})$ dependence nor the size of the changes in R_m are reproduced accurately on these assumptions. The truth lies somewhere in between the two extreme situations just considered: The magnetization in the bulk of TbFe is probably oriented, in a

vertically nonuniform manner, at $\theta(z)$ such that $0° \leqslant |\theta(z)| \leqslant |\alpha \pm 180°|$. As a matter of fact, an excellent agreement between experimental data and simulations can be obtained if one assumes that the hFi layer still contains at the end of cooling the very same partial iDW as formed at room temperature under $\mathbf{H}_{cf}$, unchanged but quenched. The solid line in Fig. 5(b) was computed on this assumption, using the original model of Ref. 9 to determine the H_{cf}-dependent magnetic profile $\theta(z)$ in TbFe, away from the interface. This successful assumption is also the one we made in all the simulations of the $R(H)$ and $R(\psi)$ curves collected in experiments of type I (Fig. 3).

It is worth noting that the theoretical $R_m(H_{cf})$ dependence is rather robust against little changes in the room temperature magnetic parameters of TbFe,[9] hence against moderate variations in the hFi micromagnetic structure. Therefore, drawing conclusions regarding the precise shape of the quenched iDW from the $R_m(H_{cf})$ data seems hazardous. The presence of the iDW and the fact that its thickness diminishes with increasing H_{cf} are all that can be ascertained from the analysis above.

The fact that the magnetization profile in TbFe does not change significantly upon cooling, although its (local) anisotropy increases tremendously, may appear as surprising. However, it has been clearly established in independent experiments of polarized neutron reflectivity.[15] Our current understanding of this phenomenon is the following. The strong magnetic rigidity of the amorphous TbFe alloy at 20 K arises from the single-ion anisotropy of Tb. The latter is locally uniaxial but oriented almost randomly in space, due to the lack of crystalline and chemical order in the material. As a result, TbFe is not an ideal ferrimagnet as GdFe; it is a sperimagnet.[27,28] Standing alone, TbFe possesses at elevated temperature a multiplicity of different, nearly degenerated magnetic configurations separated from one another by a series of energy barriers.[28] When cooled in an external field, a particular configuration (the thermoremanent state) with a large spontaneous moment in the direction of the field is singled out and gets progressively quenched as the local anisotropy increases. If the TbFe alloy, having the form of a thin film, is exchange coupled to another magnetized material (GdFe here), the selected configuration may be one in which the spontaneous moment is twisted through the thickness, as a result of the competition between the Zeeman and interfacial exchange interactions. As it does not favor any particular macroscopic direction, the increase in local anisotropy during cooling does not strongly affect the overall orientation of the magnetization (it might give rise to enhanced spatial fluctuations of magnetization orientation on an atomic length scale, though). However, it progressively enhances the height of the energy barriers mentioned before, thus contributing in blocking the magnetization further.

B. Exchange-bias properties versus cooling field angle

1. Exchange-bias field and pinning angle

Further conclusive indications that a partial iDW is quenched in TbFe are provided by the results of the experiments of type II. As may be seen in Fig. 6(a), the exchange-bias field exhibits two distinct variations as a function of the cooling field orientation depending on the handedness of the iDW formed prior to cooling. Interestingly, these two variations are similar and can be deduced from one another by translation along the ψ_{cf} axis by an angle 2Λ, with $\Lambda = 28°$. Similarly, the pinning angle is found to be, in both cases, an almost linear function of the cooling field angle, but with axis intercepts that differ by 2Λ [Fig. 6(b)].

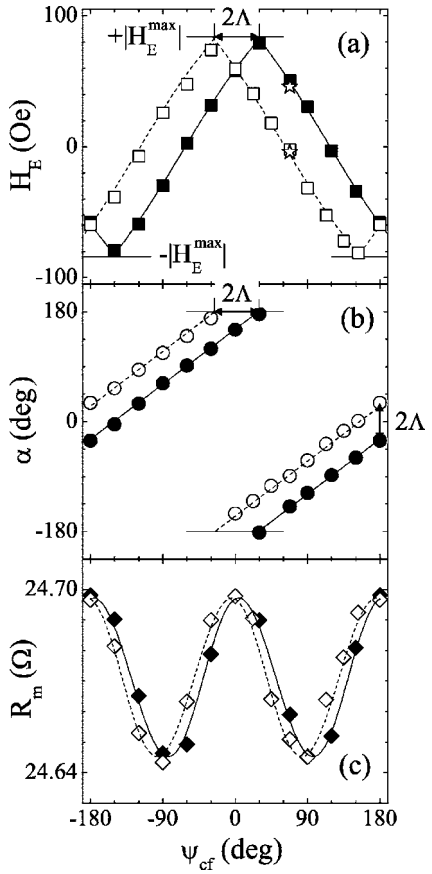

FIG. 6. Variation of the exchange-bias field H_E (a), pinning angle α (b), and maximum resistance R_m (c) as a function of the cooling field angle ψ_{cf} (experiments of type II), at 20 K, after formation of a left handed iDW (open symbols) or of a right handed iDW (solid symbols) at room temperature. The lines in (a), (b), and (c) are, respectively, guides to the eye, linear fits to the experimental data, and theoretical predictions. The stars in (a) correspond to the exchange-bias fields of the double AMR loops discussed in Sec. IV B 3.

Let us consider the case where a left handed iDW was formed at high temperature. In this case, we find experimentally that $\alpha = \psi_{cf} + \Lambda \pm 180°$ [Fig. 6(c)]. Moreover, we know that, due to the antiferromagnetic nature of the interfacial coupling, the pinning direction must be antiparallel to the interface hFi magnetization, hence $\alpha = \theta^i_{\mathrm{TbFe}} \pm 180°$. Thus, we can deduce that the frozen interface hFi magnetization is oriented at a positive angle Λ from the cooling field ($\theta^i_{\mathrm{TbFe}} = \psi_{cf} + \Lambda$), whatever be ψ_{cf}. On the other hand, given the large thickness of the TbFe layer and magnitude of the cooling field, and in agreement with the $R_m(\psi_{cf})$ data (see Sec. IV B 2), we expect that the frozen hFi magnetization at the

free TbFe/capping-layer interface be aligned close to the cooling field direction. Then, we can finally conclude from the $H_E(\psi_{cf})$ dependence that a left handed partial iDW of angular span close to Λ is very likely frozen in TbFe. A similar reasoning leads to the conclusion that a partial iDW with the same angular span but of opposite (right) handedness is frozen in TbFe after a right handed iDW has been formed at room temperature ($\alpha=\psi_{cf}-\Lambda\pm180°$, $\theta^i_{\mathrm{TbFe}}=\psi_{cf}-\Lambda$). Of course, Λ ought to depend on H_{cf}, in agreement with the variation of R_m with H_{cf} (see Sec. IV A 2).

2. Maximum resistance

In experiments of type II, unlike in experiments of type I (Sec. IV A), the changes in the maximum resistance R_m are strongly dominated by large modifications in the orientation of the TbFe magnetization [Fig. 6(c)]. Indeed, if no such modification occurred, the peak-to-peak change in R_m upon variation of ψ_{cf} between $-180°$ and $+180°$, ΔR_m, would only be 7 mΩ (as calculated with $\rho_\perp=\rho_\parallel$ for TbFe), which is much smaller than observed experimentally ($\Delta R_m\sim52$ mΩ). The shape of the $R_m(\psi_{cf})$ dependencies and the position of their extrema indicate that the frozen TbFe magnetization is always oriented close to the cooling field direction. Yet, ΔR_m is slightly less than it would be (58 mΩ) if the TbFe magnetization were uniform across the layer thickness and pointed at $\theta(z)=\psi_{cf}$ (except at the interface, of course, where $\theta^i_{\mathrm{TbFe}}=\alpha\pm180°\neq\psi_{cf}$). This result shows that TbFe presents some spread in its magnetization distribution and constitutes one more signature of the presence of a quenched iDW.

As H_E and α, R_m shows distinct, though similar, variations with ψ_{cf} depending on the chirality of the iDW selected at room temperature. This time, too, the data sets associated with the two handedness can be (approximately) deduced from one another by translation along the ψ_{cf} axis. Here, however, the angle shift, $2\psi_m$ (with $\psi_m\simeq6°$), does not amount to twice the angle of the interface TbFe magnetization with respect to $\mathbf{H}_{cf}$, 2Λ. It is rather an estimate of twice the angle of the TbFe magnetization with respect to $\mathbf{H}_{cf}$ averaged throughout the whole TbFe slab, i.e., twice the mean magnetization angle $\langle\theta(z)-\psi_{cf}\rangle$ in the quenched iDW. Thereby, it is not surprising that ψ_m be smaller than Λ.

The experimental $R_m(\psi_{cf})$ data [Fig. 6(c)] and, more generally, all of the AMR data collected in experiments of type II could be reproduced accurately on the assumption that the magnetic profile frozen in the bulk of the hFi slab is the one formed at room temperature in an external field of 10 kOe applied along $+\hat{\mathbf{u}}$ (as predicted by the model of Ref. 9), simply rotated by the angle ψ_{cf}. This point and the fact that $\theta^i_{\mathrm{TbFe}}-\psi_{cf}$ is found approximately independent of ψ_{cf} corroborate the statement we made earlier (Sec. III A) saying that the magnetic configuration formed at room temperature in TbFe is rotated in a block-wise manner, i.e., without its shape being significantly modified, when the applied field of 10 kOe is brought from approximately parallel to $+\hat{\mathbf{u}}$ ($\psi=\epsilon$) to its angular position during cooling ψ_{cf}.

3. Double AMR loops

On one occasion during the series of experiments of type II, data were collected which could not be modeled using our one-dimensional micromagnetic approach. In this particular experiment, in which the cooling field was applied at $\psi_{cf}=+68°$, the sample exhibited double AMR loops (Fig. 7). The individual loops were shifted along the field axis in opposite directions, negatively for one of them, positively for the other, and by amounts that differed in their absolute values, too. Attempts were made to reproduce this result following scrupulously the experimental procedure described in Sec. III A. These failed: Single loops were systematically obtained, which were shifted negatively ($H_E=-4$ Oe) or positively ($H_E=+46$ Oe) depending on whether the frozen iDW was left handed or right handed (Fig. 7).

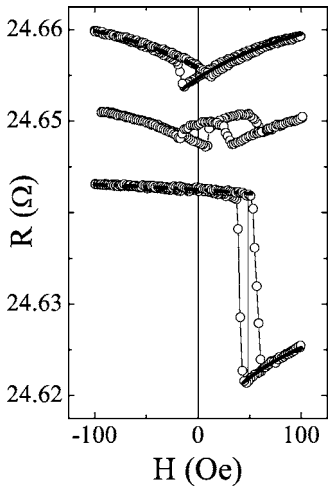

FIG. 7. AMR loops obtained for $\psi_{cf}=+68°$ (experiment of type II) after quenching of a left handed iDW (top), a right handed iDW (bottom), and a lateral multi-domain structure in TbFe (center). For convenience, the topmost and bottommost loops have been shifted vertically by +9 and −16 mΩ, respectively. As in Fig. 3, the thick solid and dashed lines are the theoretical AMR data corresponding to the magnetic configurations of type ε^+ and ε^-, respectively.

Interestingly, the exchange-bias fields of these single loops are extremely close to those of the double loops [Fig. 6(a)]. This indicates that, in the particular experiment where the double loops were observed, the TbFe layer was most certainly quenched in a lateral multi-domain state, consisting of a mixture of regions containing left handed iDW *and* right handed iDW. The observation of double loops also reveals that averaging of the exchange-bias effect did not occur over the sample. This required that the different domains in TbFe behave more or less independently of each other and that their size be large as compared to the characteristic lateral size of the domains in GdFe.[8,29] The situation encountered here is thus somewhat similar to that found in field-cooled $\mathrm{CoO}/[\mathrm{Co}/\mathrm{Pt}]_2/\mathrm{Co}/\mathrm{Ru}/[\mathrm{Co}/\mathrm{Pt}]_{10}$ stacks[29] and $\mathrm{TM}/\mathrm{FeF}_2$ bilayers[8] (where TM is Fe, Co, or Ni) at the transition from NEB to PEB, or in NiFe/FeMn (Ref. 30) and $\mathrm{TM}/\mathrm{FeF}_2$ (Refs. 8 and 31) F/AF bilayers cooled in zero field with the F layer in a multi-domain magnetic state.

It is hardly possible to determine the fractions of the TbFe layer occupied by the two kinds of regions from the AMR data. Nevertheless, from the relative size of the individual loops, we can infer that the domains with left handed iDW were certainly present in larger proportion, being bigger

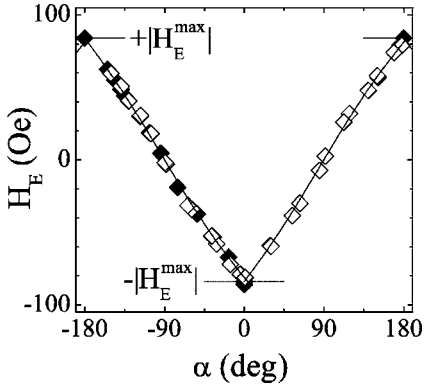

FIG. 8. Exchange-bias field H_E as a function of pinning angle α. Solid and open symbols correspond to data from experiments of type I and type II, respectively. The line is the theoretical prediction.

and/or more numerous, than those containing right handed iDW. The only explanation for the splitting of TbFe in a multi-domain structure we can propose is an accidental perfect alignment of the magnetic field along the easy axis of GdFe (not favoring a particular iDW handedness) at the very beginning of the experiment, i.e., when the noncolinear interface magnetic structure formed.

C. Exchange-bias field versus pinning angle

The results of the 40 experiments (types I and II altogether) carried out for the present study can be summarized in the form of a plot of the exchange-bias field as a function of the pinning angle (Fig. 8). This plot reveals most clearly the correlation that exists between the size of the GdFe hysteresis loop shift and the orientation of the interface TbFe magnetization ($\theta^i_{\mathrm{TbFe}}=\alpha\pm180°$): The latter entirely determines the former, irrespective of whether the latter is realized by adjusting the magnitude of the cooling field, its orientation, or both of them. Obviously, as far as H_E is concerned, the details of the micromagnetic structure in the bulk of TbFe are not relevant, only the orientation of its magnetization at the interface matters.

As may be seen in Fig. 8, H_E varies almost linearly with $|\alpha|$, between the two extreme values of $-|H_E^{max}|$ and $+|H_E^{max}|$ associated with $\alpha=0°$ and $|\alpha|=180°$, respectively. Such variation is not expected from simple models of exchange bias.[32] However, as most magnetic properties of the GdFe/TbFe system, it is well reproduced by the calculations, provided one chooses as a definition of H_E the exact magnetic field at which the ε^+ and ε^- equilibrium configurations of GdFe have even total energies and their relative stability reverses (see Sec. III C). In the determination of this field, the intensity of the coupling across the GdFe/TbFe interface (J) plays only a minor role. Apart from α, H_E is mostly determined by the magnetic parameters (A, K, and M) of the soft material. Then, as suggested also graphically in Fig. 4(a), the characteristic energy which controls exchange bias in our sFi/hFi system is the planar domain wall energy in the sFi material. Of course, this is so because (and as long as) the hFi magnetization is sufficiently rigid so as to remain essentially unaffected upon external field cycling and sFi magnetization reversal.

The pinning angle determines the exchange-bias field in a way which has very much to do with simple geometry, as we shall argue now. It is for $\alpha=0°$ and $|\alpha|=180°$ that the ε^+ and ε^- equilibrium configurations of GdFe are the more dissimilar. For simplicity, let us concentrate on the case where $\alpha=0°$ [Fig. 3(a)]. In the ε^- configuration, which is unstable in the absence of applied field, the GdFe layer contains a full 180° planar Bloch-like wall [Fig. 4(a)]. Its total energy is made up of important contributions from the anisotropy and exchange energy terms. Therefore, it is large whatever H is. In contrast, the ε^+ configuration shows no magnetization twist and its total energy consists entirely of Zeeman energy. It takes a large (negative) field opposite to the magnetization of GdFe to make ε^+ become as energetic as ε^-, hence the large exchange-bias field. For $|\alpha|=90°$, which is nearly the case in Figs. 3(c) and 4(b), both ε^+ and ε^- configurations are stable in the absence of external field; ε^+ and ε^- are very much alike and consist of strongly twisted magnetic profiles. In fact, for geometrical reasons, ε^+ and ε^- are mirror symmetric from one another about the pinning direction $\hat{\mathbf{a}}$ and hard axis of magnetization. Thus, their total magnetic energies contain identical contributions from the exchange and anisotropy terms and are strictly equal, in zero applied field. This is the reason why H_E is nil.

D. Coercivity

Coercivity is an issue that we have deliberately left aside so far in this paper. We shall discuss it now. In many F/AF bilayer systems, exchange-bias is associated with modifications in the coercive field H_C of the pinned F layer, as compared to that of a free F layer. Specifically, H_C is usually enhanced, as a result of the interaction with the adjacent antiferromagnet. Moreover, it often exhibits drastically modified variations with, for instance, the angle of the cycling field.[33] In the GdFe/TbFe system, too, the exchange coupling (to TbFe) across the interface affects the coercivity of the exchange-biased (GdFe) layer.

As observed for other multilayered structures showing a transition from NEB to PEB with increasing cooling field, such as Fe/MnF_2 (Ref. 7) and GdFe/NiCoO (Ref. 34) bilayers, or $[Pt/Co]_{10}/Ru/[Co/Pt]_3/Co/CoO$ stacks,[29] coercivity in GdFe/TbFe exhibits a pronounced maximum as the exchange-bias field goes through zero and changes sign [Fig. 9(a) and Ref. 9]. Here, interestingly, H_C is also found to exhibit well defined maxima in its variation as a function of the cooling field angle [Fig. 9(b)]. In all cases, these maxima correspond to situations where $|\alpha|$ amounts to 90° [Figs. 9(c) and 9(d)]. However, neither the global shape of the $H_C(\alpha)$ dependence nor the size of the changes in H_C with α are the same for the two types of experiments (I and II) we performed. Then, unlike H_E, which is uniquely determined by the orientation of the TbFe magnetization at the interface, hence by α (see Sec. IV C), H_C does depend both on the pinning angle *and* on the shape of the partial iDW quenched in TbFe.

Explanations can be proposed as to the origin of the $H_C(\alpha)$ dependence. However, these are rather speculative. A

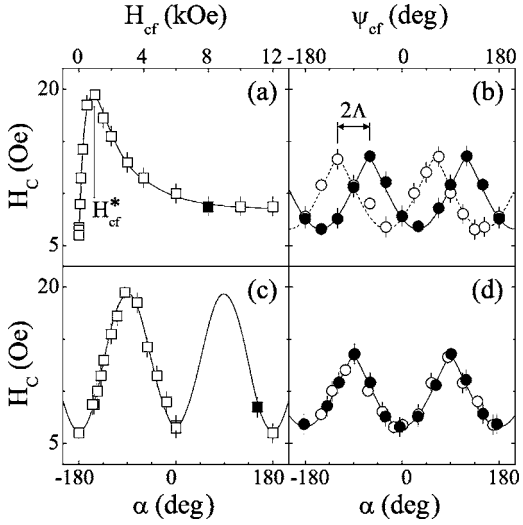

FIG. 9. Coercive field H_C as a function of the cooling field magnitude H_{cf} (a), cooling field angle ψ_{cf} (b), and pinning angle α (c) (d), at 20 K. Squares and circles correspond to data from experiments of type I and type II, respectively. Open and solid symbols correspond to cases where the quenched iDW was of left handedness and right handedness, respectively. The lines are guides to the eye.

close inspection of Fig. 3(c) allows one to verify that, even far away from the main transitions, the decreasing-field branch and the increasing-field branch of the $R(H)$ loops do not always superimpose perfectly, although the loops are completely closed. We consider this feature as an indication that the TbFe magnetization slightly rearranges as the external field is cycled. These rearrangements likely consist of rotations, no larger than a few degrees and restricted to the vicinity of the interface. With the exception of the very first of them, not discussed here (see Sec. III A), the rearrangements are fairly reproducible from one cycle to the next. The differences observed in the curvature of the increasing and decreasing field branches and the closeness of the loops suggest that the pinning direction $\hat{\mathbf{a}}$ moves back and forth around its average position, which is at the angle α determined from the $R(\psi)$ data. It is remarkable that the phenomenon in question is undetectable for $\alpha=0°$ and $|\alpha|=180°$ and is the most pronounced when $|\theta^i_{\mathrm{TbFe}}|$ is close to 90°, that is, when the torque exerted on the interface TbFe magnetization during the reversal of GdFe is the largest.[9] This reinforces our conviction that the rearrangements are provoked by the reversal of GdFe rather than by the direct interaction of the TbFe magnetization with the sweeping external field.

Thus, one possible explanation for the variation of H_C with α requires to go beyond the approximation we made up to now of a static TbFe magnetization. We propose that tiny cyclic changes in the micromagnetic structure of TbFe, possibly dependent on the shape of the frozen iDW, could result in back and forth movements of the interfacial pinning direction and, thereby, be the source of a coercivity enhancement. In essence, this is equivalent to the rotatable anisotropy often considered in F/AF systems.[17,35,36]

Before concluding, we wish to mention that lateral domain walls could also play a role in the variation of H_C with α, just as they proved to play a predominant role in other exchange coupled GdFe/TbFe bilayers.[25] The transition from the ε^+ state to the ε^- one (or vice versa) most likely occurs through the formation of reversed domains of ε^- configuration in the nonswitched ε^+ phase. These must necessarily be delineated by lateral domain walls in which the magnetization direction varies not only with the perpendicular-to-plane z coordinate, but also with the in-plane x and y coordinates. The shape of these walls must necessarily depend on the interfacial pinning angle. Therefore, α surely determines their energy cost and maybe their pinning on defects. Either way, α could affect H_C to a certain extent. Three-dimensional micromagnetic calculations would be required in order to put this possibility to the test.

V. CONCLUSION

Exchange-bias has been studied experimentally in an amorphous soft/hard ferrimagnetic/ferrimagnetic $Gd_{40}Fe_{60}(100\ \mathrm{nm})/Tb_{12}Fe_{88}(50\ \mathrm{nm})$ bilayer. A partial interface domain wall has been shown to freeze in the TbFe pinning layer upon field cooling. Its presence manifests spectacularly: Two exchange-bias field values are generally associated with a given orientation of the cooling field. These correspond to the two possible handedness of the frozen wall. With increasing cooling field magnitude, the thickness of the partial wall diminishes and the interface TbFe magnetization rotates progressively, in the plane of the film, towards the cooling field direction. This gives rise to an intrinsically continuous transition from negative exchange bias to positive exchange bias.

The present study thus shows a new example of a situation in which the direction of unidirectional anisotropy is not necessarily that of the cooling field $\mathbf{H}_{cf}$; It may be oriented at any angle, be perpendicular or even antiparallel to $\mathbf{H}_{cf}$. In the studied system, this is so essentially as a result of a competition between the antiferromagnetic interfacial exchange interaction and the Zeeman interaction. In other systems, such as $Co/Fe_xZn_{1-x}F_2$,[37] it is the combined effect of a strong uniaxial anisotropy and of a twinned crystallographic structure of the AF material which may lead to such a situation.

In the $Gd_{40}Fe_{60}/Tb_{12}Fe_{88}$ system, the maximum value of the exchange-bias field $|H_E^{max}|$ is determined by the energy of a 180° planar domain wall in the soft GdFe alloy. Any particular exchange-bias field value between $-|H_E^{max}|$ and $+|H_E^{max}|$ can be achieved, in an infinite number of different ways, by adjusting the amplitude and the orientation of the cooling field, as well as by selecting the chirality of the quenched wall. However, H_E is uniquely determined by the angle of the interface magnetization of TbFe. Therefore, tuning H_E simply amounts to controlling the interface magnetization of the pinning layer. Unlike the exchange-bias field, the coercivity of the pinned layer does depend on the micromagnetic structure deeper in the pinning layer.

ACKNOWLEDGMENTS

The authors thank D. Pierre and D. Ligiardi for sample preparation, and L. Joly for assistance with the computer calculations.

*Electronic address: yves.henry@ipcms.u-strasbg.fr

[1] J. Nogués, D. Lederman, T. J. Moran, and I. K. Schuller, Phys. Rev. Lett. **76**, 4624 (1996).
[2] J. Nogués, D. Lederman, T. J. Moran, I. K. Schuller, and K. V. Rao, Appl. Phys. Lett. **68**, 3186 (1996).
[3] J. Nogués and I. K. Schuller, J. Magn. Magn. Mater. **192**, 203 (1999).
[4] A. E. Berkowitz and K. Takano, J. Magn. Magn. Mater. **200**, 552 (1999).
[5] C. Leighton, J. Nogués, H. Suhl, and I. K. Schuller, Phys. Rev. B **60**, 12837 (1999).
[6] J. Nogués, C. Leighton, and I. K. Schuller, Phys. Rev. B **61**, 1315 (2000).
[7] C. Leighton, J. Nogués, B. J. Jönsson-Åkerman, and I. K. Schuller, Phys. Rev. Lett. **84**, 3466 (2000).
[8] I. V. Roshchin, O. Petracic, R. Morales, Z.-P. Li, X. Battle, and I. K. Schuller, Europhys. Lett. **71**, 297 (2005).
[9] S. Mangin, F. Montaigne, and A. Schuhl, Phys. Rev. B **68**, 140404(R) (2003).
[10] D. Mergel, J. Appl. Phys. **74**, 4072 (1993).
[11] S. Mangin, C. Bellouard, G. Marchal, and B. Barbara, J. Magn. Magn. Mater. **165**, 161 (1997).
[12] F. Canet, S. Mangin, C. Bellouard, and M. Piecuch, Europhys. Lett. **52**, 594 (2000).
[13] R. Morales, J. I. Martín, and J. M. Alameda, Phys. Rev. B **70**, 174440 (2004), and references therein.
[14] These changes never exceeded a few mΩ and are to be compared with the 58 mΩ change in resistance that a block-wise rotation of the TbFe magnetization from parallel to perpendicular to the current would have produced.
[15] T. Hauet, J. A. Borcher, Ph. Mangin, Y. Henry, and S. Mangin, Phys. Rev. Lett. **96**, 067207 (2006).
[16] B. H. Miller and E. D. Dahlberg, Appl. Phys. Lett. **69**, 3932 (1996).
[17] R. D. McMichael, M. D. Stiles, P. J. Chen, and W. F. Egelhoff, Jr., Phys. Rev. B **58**, 8605 (1998).
[18] S. Wüchner, J. C. Toussaint, and J. Voiron, Phys. Rev. B **55**, 11576 (1997), and references therein.
[19] K. Mibu, T. Nagahama, and T. Shingo, J. Magn. Magn. Mater. **163**, 75 (1996).
[20] E. E. Fullerton, J. S. Jiang, M. Grimsditch, C. H. Sowers, and S. D. Bader, Phys. Rev. B **58**, 12193 (1998).
[21] T. Nagahama, K. Mibu, and T. Shingo, J. Phys. D **31**, 43 (1998).
[22] F. Montaigne, S. Mangin, and Y. Henry, Phys. Rev. B **67**, 144412 (2003).
[23] A. Bill and H. B. Braun, J. Magn. Magn. Mater. **272-276**, 1266 (2004).
[24] In this paper, wherever a ± symbol appears in the expression of an angle, it is to be replaced by the sign + or by the sign − whichever is necessary so that the angle in question belongs to the interval $[-180°, +180°]$.
[25] Y. Henry, S. Mangin, and F. Montaigne, Phys. Rev. B **69**, 140401(R) (2004).
[26] F. Montaigne, T. Hauet, Y. Henry, and S. Mangin (unpublished).
[27] J. M. D. Coey, J. Appl. Phys. **49**, 1646 (1978).
[28] K. Moorjani and J. M. D. Coey, *Magnetic Glasses* (Elsevier, Amsterdam, 1984), Chap. VI.
[29] T. L. Kirk, O. Hellwig, and E. E. Fullerton, Phys. Rev. B **65**, 224426 (2002).
[30] N. J. Gökemeijer, J. W. Cai, and C. L. Chien, Phys. Rev. B **60**, 3033 (1999).
[31] P. Miltényi, M. Gierlings, M. Bamming, U. May, G. Güntherodt, J. Nogués, M. Gruyters, C. Leighton, and I. K. Schuller, Appl. Phys. Lett. **75**, 2304 (1999).
[32] W. P. Meiklejohn and C. P. Bean, Phys. Rev. **102**, 1413 (1956); **105**, 904 (1957).
[33] T. Ambrose, R. L. Sommer, and C. L. Chien, Phys. Rev. B **56**, 83 (1997).
[34] D. Z. Yang, J. Du, L. Sun, X. S. Wu, X. X. Zhang, and S. M. Zhou, Phys. Rev. B **71**, 144417 (2005).
[35] L. Wee, R. L. Stamps, L. Malkinski, and Z. Celinski, Phys. Rev. B **69**, 134426 (2004).
[36] J. McCord, R. Mattheis, and D. Elefant, Phys. Rev. B **70**, 094420 (2004).
[37] H. Shi and D. Lederman, Phys. Rev. B **66**, 094426 (2002).